Mitochondria-related male infertility

Kazuto Nakada*†‡§, Akitsugu Sato*†¶, Kayo Yoshida‖, Takashi Morita‖, Hiromitsu Tanaka, Shin-Ichi Inoue*, Hiromichi Yonekawa*¶, and Jun-Ichi Hayashi***

*Graduate School of Life and Environmental Sciences and †Center for Tsukuba Advanced Research Alliance, University of Tsukuba, 1-1-1 Tennoudai, Tsukuba, Ibaraki 305-8572, Japan; ‡Precursory Research for Embryonic Science and Technology, Japan Science and Technology Agency, Kawaguchi, Saitama 332-0012, Japan; ¶Department of Laboratory Animal Science, Tokyo Metropolitan Institute of Medical Science, 3-18-22 Honkomagome, Bunkyo-ku, Tokyo 113-8613, Japan; ‖Department of Molecular Genetics, Osaka City University, Graduate School of Medicine, 1-4-3 Asahimachi, Abeno-ku, Osaka 545-8585, Japan; and **Department of Science for Laboratory Experimentation, Research Institute for Microbial Diseases, Osaka University, 3-1 Yamadaoka, Suita City, Osaka 565-0871, Japan

Edited by Ryuzo Yanagimachi, University of Hawaii, Honolulu, HI, and approved August 17, 2006 (received for review June 4, 2006)

Approximately 15% of human couples are affected by infertility, and about half of these cases of infertility can be attributed to men, through low sperm motility (asthenozoospermia) or/and numbers (oligospermia). Because mitochondrial genome (mtDNA) mutations are identified in patients with fertility problems, there is a possibility that mitochondrial respiration defects contribute to male infertility. To address this possibility, we used a transmitochondrial mouse model (mito-mice) carrying wild-type mtDNA and mutant mtDNA with a pathogenic 4,696-bp deletion (ΔmtDNA). Here we show that mitochondrial respiration defects caused by the accumulation of ΔmtDNA induced oligospermia and asthenozoospermia in the mito-mice. Most sperm from the infertile mito-mice had abnormalities in the middle piece and nucleus. Testes of the infertile mito-mice showed meiotic arrest at the zygotene stage as well as enhanced apoptosis. Thus, our *in vivo* study using mito-mice directly demonstrates that normal mitochondrial respiration is required for mammalian spermatogenesis, and its defects resulting from accumulated mutant mtDNAs cause male infertility.

meiosis | mitochondrial diseases | model mice | respiration defects | spermatogenesis

Mitochondria have their own genome, mtDNA, and most cells in the body contain between 10^3 and 10^4 copies of mtDNA. Mammalian mtDNA encodes 13 polypeptides that are essential subunits for electron transport complexes on the inner mitochondrial membrane and 22 tRNAs and 2 rRNAs that are necessary for the translation of these 13 polypeptides. The accumulation of pathogenic mtDNAs having large-scale deletion or point mutation and the resultant mitochondrial respiration defects are associated with a wide variety of disorders, such as mitochondrial diseases, neurodegenerative diseases, and diabetes, as well as aging (for review, see ref. 1). Reduced sperm motility has been reported in patients with mitochondrial diseases (2, 3), and pathogenic mutant mtDNA has also been identified in semen samples of patients with fertility problems (4–6), although the accumulation of mutant mtDNA in semen samples is insufficient for the induction of mitochondrial respiration defects. Considering that sperm motility depends on mitochondrial respiratory function (7), these findings from human studies predict that the accumulation of pathogenic mutant mtDNA and the resultant mitochondrial respiration defects contribute to sperm dysfunction, probably leading to male infertility. By using mice with the disrupted expression of glyceraldehyde-3-phosphate dehydrogenase-S, a sperm-specific glycolytic enzyme, however, it has been implied that most of the energy required for sperm motility is generated by glycolysis rather than mitochondrial oxidative phosphorylation (8). Moreover, it is possible that nuclear DNA mutations were involved in the expression of respiration defects in all of these cases because respiratory function is controlled by both nuclear DNA and mtDNA (for review, see ref. 1). Thus, there is as yet no convincing experimental evidence showing that mitochondrial respiration defects induced by accumulated mutant mtDNA result in male infertility.

For resolving the problem, transmitochondrial mice (mito-mice) carrying both pathogenic ΔmtDNA, which has a 4,696-bp deletion from nucleotide position 7,759 in the $tRNA^{Lys}$ gene to position 12,454 in the *ND5* gene, and wild-type mtDNA are a suitable model system (9). ΔmtDNA is similar to pathogenic mutant mtDNA with the common deletion in human mitochondrial diseases (10). When mito-mice were generated by introduction of mitochondria carrying ΔmtDNA into zygotes of C57BL/6J (B6) mice, these mice carrying >80% mtDNA showed mitochondrial respiration defects and the resultant mitochondrial diseases (9, 11, 12). The great advantages of mito-mice are that they all share exactly the same nuclear genomic background, and their genetic variation is restricted to the proportions of the introduced pathogenic ΔmtDNA. Therefore, mito-mice have provided direct evidence that mitochondrial respiration defects induced by the accumulation of ΔmtDNA are sufficient by themselves for expression of the clinical phenotypes observed in patients with mutated mtDNA.

Mammalian spermatogenesis occurs continuously with individual maturation of sperm and comprises the entire sequence of events by which spermatogonia are transformed into sperm, through meiotic division of spermatocytes. In yeast, it has been reported that mitochondrial function is essential for meiosis (13–15) and the meiotic sporulation process (16). In mammalian spermatogenesis, however, it has not been well understood whether mitochondrial respiratory function is essential for the meiotic process because there was no effective animal model for answering the fundamental question.

In this work, we investigated male infertility in mito-mice (4.5–6.5 months old) carrying different proportions of ΔmtDNA compared with that in age-matched B6 mice as normal controls, and we showed that pathogenic mtDNA-derived mitochondrial respiratory defects are responsible for oligospermia and asthenozoospermia. Furthermore, our study demonstrated that the mitochondrial respiration defects gave rise to meiotic arrest and abnormalities of sperm morphology, showing the requirements of mitochondrial respiratory function in mammalian spermatogenesis.

Results

To select the mito-mice used for this work, we deduced the proportions of ΔmtDNA in tissues of 4.5- to 5.0-month-old male

Author contributions: K.N. and A.S. contributed equally to this work. K.N., T.M., H.Y., and J.-I.H. designed research; K.N., A.S., and K.Y. performed research; K.Y., T.M., and H.T. contributed new reagents/analytic tools; K.N., A.S., K.Y., and S.-I.I. analyzed data; and K.N. wrote the paper.

The authors declare no conflict of interest.

This paper was submitted directly (Track II) to the PNAS office.

Abbreviations: COX, cytochrome *c* oxidase; ΔmtDNA, mutant mtDNA with a pathogenic 4,696-bp deletion; MCA, male metaphase chromosome-associated acidic protein (meichroacidin); mito-mice, transmitochondrial mice; SC, synaptonemal complex.

§To whom correspondence should be addressed at: Graduate School of Life and Environmental Sciences, University of Tsukuba, Tennoudai, Tsukuba, Ibaraki 305-8572, Japan. E-mail: knakada@sakura.cc.tsukuba.ac.jp.

www.pnas.org/cgi/doi/10.1073/pnas.0604641103

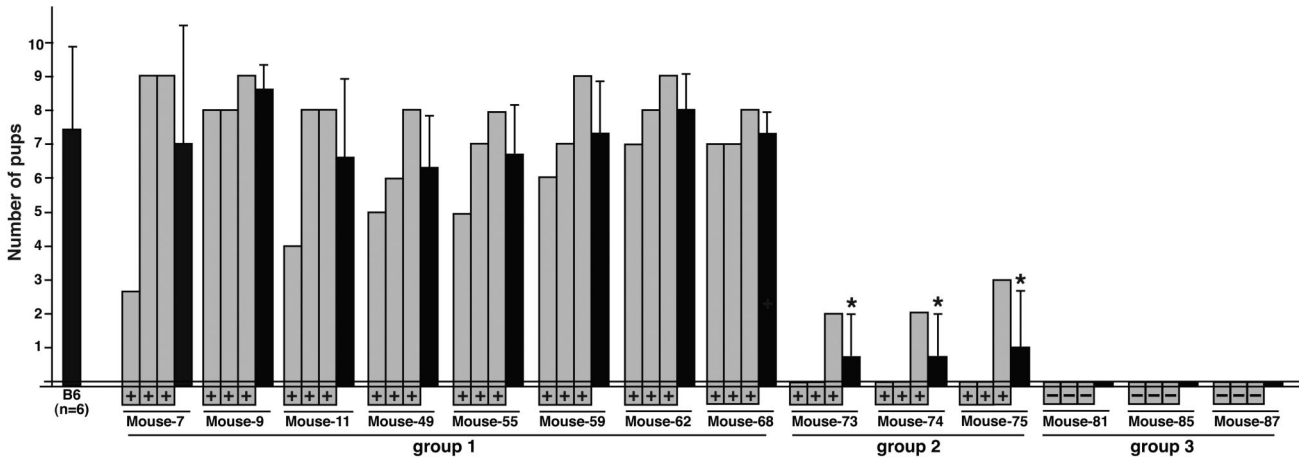

Fig. 1. Effect of accumulated ΔmtDNA in mito-mice. A mating assay of mito-mice is shown. Normal B6 mice ($n = 3$) and mito-mice carrying 7.0% (mouse-7), 8.6% (mouse-9), 11.1% (mouse-11), 48.8% (mouse-49), 54.6% (mouse-55), 59.4% (mouse-59), 62.0% (mouse-62), 68.0% (mouse-68), 73.3% (mouse-73), 73.9% (mouse-74), 75.2% (mouse-75), 81.3% (mouse-81), 84.8% (mouse-85), and 86.6% (mouse-87) ΔmtDNA in their tails were used in this assay. The presence or absence of copulation plugs is shown as + or −, respectively. Copulation plugs were not found in the females paired with mouse-81, -85, and -87. Mito-mice carrying ≥73.3% ΔmtDNA in their tails had reduced numbers of progeny. Black bars show the means ± SD. Asterisks indicate significant differences ($P < 0.05$).

mito-mice from tail samples (see Table 1, which is published as supporting information on the PNAS web site) without having to kill the mice because the proportions are approximately uniform throughout the tissues of individual mito-mice (9, 11, 17). Based on the deduced proportions of ΔmtDNA, we classified the mito-mice into three groups (Fig. 1): mito-mice carrying ≤68% ΔmtDNA (group 1), those carrying 70–80% ΔmtDNA (group 2), and those carrying ≥81% ΔmtDNA (group 3). Group 1 mito-mice were quite normal, and they showed no phenotypes of mitochondrial diseases, although they carried a maximum of 68% ΔmtDNA. Group 2 mito-mice were apparently healthy, but they showed a slight mitochondrial respiratory deficiency and lactic acidosis after glucose loading. Group 3 mito-mice showed systemic mitochondrial respiration defects and the resultant mitochondrial disease phenotypes, such as low body weight, lactic acidosis, myopathy, heart block, renal failure, and deafness. Therefore, the group 1 mito-mice could be used as negative controls because the genetic differences of these mito-mice groups were limited to the proportions of exogenously introduced ΔmtDNA

If mutated mtDNA and the resultant mitochondrial respiration defects are responsible for male infertility, then the number of progeny from female mice mated with male mito-mice might be reduced in proportion to the ΔmtDNA load. To test this hypothesis, we carried out a mating assay using male mito-mice carrying 7.0–86.6% ΔmtDNA in their tails (groups 1–3 mito-mice) and normal male B6 mice (Fig. 1). We observed copulation plugs, showing successful mating, in all of the female mice when groups 1 and 2 mito-mice and normal B6 mice were cohabitated with female B6 mice (2–4 months old). The numbers of progeny obtained were clearly reduced in group 2, whereas there was no significant difference in the average progeny number between group 1 and B6 mice. On the other hand, even when group 3 mito-mice were cohabitated with the females for 4 weeks, we found no copulation plugs in the female mice, and we obtained no progeny. In group 3 mito-mice, we observed mitochondrial myopathy and the resultant behavior disorder, leading to mating failure (not shown).

The results of the mating assay showed that the accumulation of >73% ΔmtDNA in mito-mice was associated with male infertility, but the main reason for male infertility in group 3 mito-mice was probably behavior problems caused by mitochondrial myopathy. However, the mechanisms by which the accumulated ΔmtDNA induced male infertility in mito-mice were still not clear. To address this point, we examined the quality of sperm prepared from mito-mice. As for the mitochondrial respiratory function and morphology of sperm, we observed deficiency of cytochrome *c* oxidase (COX) activity (Fig. 2*A*) and one of the respiration chain complexes; abnormalities in the middle piece, including unevenly sterile and bending forms; and regarding the head, we observed both pyknosis and headless forms (Fig. 2*B*), most often in groups 2 and 3 mito-mice. These defects were probably the result of abnormal sperm formation and the subsequent occurrence of asthenozoospermia in groups 2 and 3 mito-mice. Actually, sperm motility was decreased in group 2 compared with group 1 mito-mice and B6 mice, and no motile sperm were observed in group 3 (Fig. 2*D*). The sperm number was also clearly decreased in groups 2 and 3 mito-mice compared with group 1 mito-mice and B6 mice, and the decrease was greater in group 3 (Fig. 2*C*). Thus, asthenozoospermia and oligospermia were present in groups 2 and 3 mito-mice.

To test whether the oligospermia and asthenozoospermia in mito-mice resulted in male infertility, we used an *in vitro* fertilization assay with sperm prepared from groups 1–3 mito-mice and normal B6 mice. In the assay, fertilization rates, measured as the developmental frequency of two-cell-stage embryos, were clearly decreased in group 2 mito-mice compared with group 1 mito-mice and B6 mice, and we observed no two-cell-stage embryos in group 3 mito-mice (Fig. 2*E*). Thus, we concluded that oligospermia and asthenozoospermia were the main causes of male infertility in group 2 and that in group 3 mito-mice, they would have led to male infertility had those mito-mice mated successfully.

The occurrence of oligospermia suggests abnormal spermatogenesis in the infertile mito-mice. In addition, sperm samples from mito-mice contained a maximum of 75.2% ΔmtDNA, even when the mito-mice carried >80% ΔmtDNA (Table 1), indicating that spermatogenic cells carrying >75.2% ΔmtDNA did not differentiate into sperm because of the mitochondrial respiratory dysfunction induced by the accumulated ΔmtDNA. To investigate how oligospermia was induced in mito-mice, we examined histological and histochemical changes in testes removed from groups 1–3 mito-mice and normal B6 mice. The numbers of spermatocytes, spermatids, and sperm were clearly decreased in the testis of mouse-75 (group 2); in the testis of mouse-85 (group 3) it was very difficult to identify any sper-

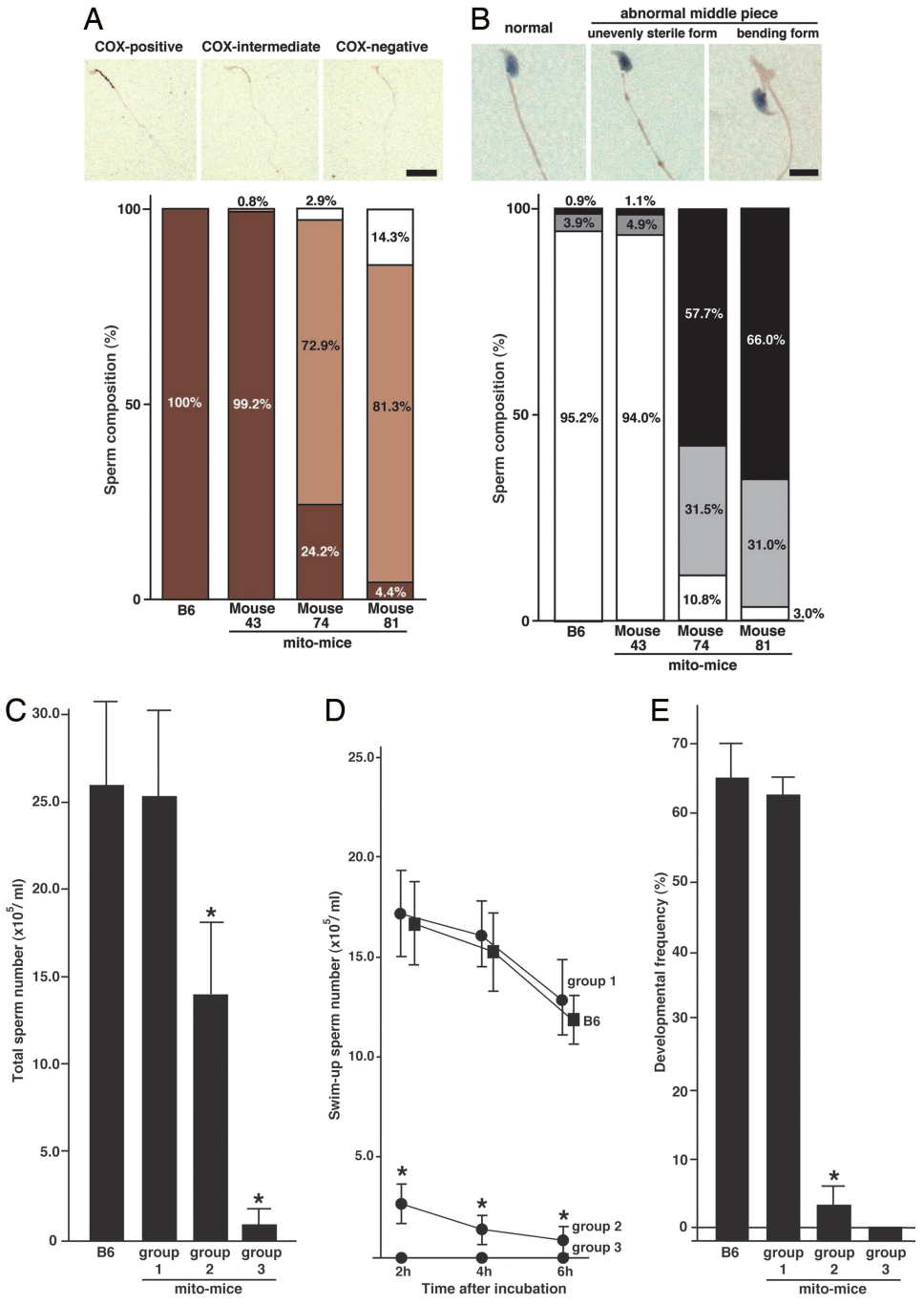

Fig. 2. Biological quality of sperm from mito-mice. (*A*) COX activity in sperm. Sperm samples from mouse-43 (group 1), -74 (group 2), -81 (group 3), and a normal B6 mouse were cytochemically stained for COX activity, and the relative frequency of COX-positive (brown), -intermediate (light brown), and -negative (white) sperm in each mouse was determined by the degree of staining. In mouse-74 and -81, frequencies of COX-intermediate and -negative sperm were higher than the frequency in the B6 mouse. (Scale bar: 30 μm.) (*B*) Morphological abnormalities in sperm. Sperm samples from mouse-43 (group 1), -74 (group 2), -81 (group 3), and a normal B6 mouse were stained with H&E, and the frequencies of morphological abnormalities in each mouse were estimated. (*Upper*) Sperm with abnormal middle pieces. Black, gray, and white indicate sperm with middle piece abnormalities, nuclear abnormalities, and normal morphology, respectively. In mouse-74 and -81, the frequencies of sperm with middle piece or nuclear abnormalities were higher than in mouse-43 and the normal B6 mouse. (Scale bar: 10 μm.) (*C*) Total number of sperm. Sperm samples collected from both sides of the cauda epididymidis of group 1 mito-mice (mouse-6, -43, and -59), group 2 mito-mice (mouse-73, -74, and -77), group 3 mito-mice (mouse-81, -85, and -87), and normal B6 mice ($n = 3$) were incubated in 500 μl of HTF medium, and the total sperm number was counted. Total sperm numbers were clearly decreased in groups 2 and 3. Values are the means ± SD. Asterisks indicate significant differences ($P < 0.05$). (*D*) Sperm motility. Sperm samples collected from both sides of the cauda epididymidis of group 1 mito-mice (mouse-6, -43, and -59), group 2 mito-mice (mouse-73, -74, and -77), group 3 mito-mice (mouse-81, -85, and -87), and normal B6 mice ($n = 3$) were incubated in 500 μl of HTF medium, and swim-up sperm numbers were counted after 2, 4, and 6 h of incubation. The swim-up sperm numbers in groups 2 and 3 were clearly decreased. Values are the means ± SD. Asterisks indicate significant differences ($P < 0.05$). (*E*) *In vitro* fertilization assay. Sperm samples collected from group 1 mito-mice (mouse-6, -43, and -59), group 2 mito-mice (mouse-73, -74, and -77), group 3 mito-mice (mouse-81, -85, and -87), and normal B6 mice ($n = 3$) were used in the assay. The developmental frequency of two-cell-stage embryos was used as the measure of successful fertilization rate. The fertilization rates in groups 2 and 3 were lower than those in group 1 and normal B6 mice. All values are the means ± SD. Asterisks indicate significant differences ($P < 0.05$).

matocytes, spermatids, or sperm (Fig. 3*A*). In these mice, however, spermatogonia could be seen in the external layer of the most seminiferous tubules, although their numbers were slightly decreased (Fig. 3*A*). COX histochemistry of the testis sections showed more mitochondrial respiration defects in mouse-75 and -85 (Fig. 3*B*). Therefore, the histological changes in testes of groups 2 and 3 mito-mice suggested that the mitochondrial respiration defects may affect meiosis, which is necessary for the transformation of diploid spermatocytes to haploid spermatids during spermatogenesis. To investigate this point, we immunostained testis sections with an antiserum for male meiotic metaphase chromosome-associated acidic protein (meichroacidin; MCA) because the MCA distributes in the cytoplasm of pachytene spermatocytes through to early round spermatids but not in the cytoplasm of other cells in the testis, and the MCA is localized around the metaphase chromosomes and spindles during the first and second meiotic divisions (18). Fewer cells stained positive for the anti-MCA decreased in mouse-75 testis than in mouse-11 or B6 mouse testes, and the number of such cells decreased further in mouse-85, indicating meiotic abnormalities in spermatogenesis (Fig. 3*C*).

Because differences in synaptonemal complexes (SCs) are used to identify each stage of the meiotic process during spermatogenesis (for review, see ref. 19), we performed a

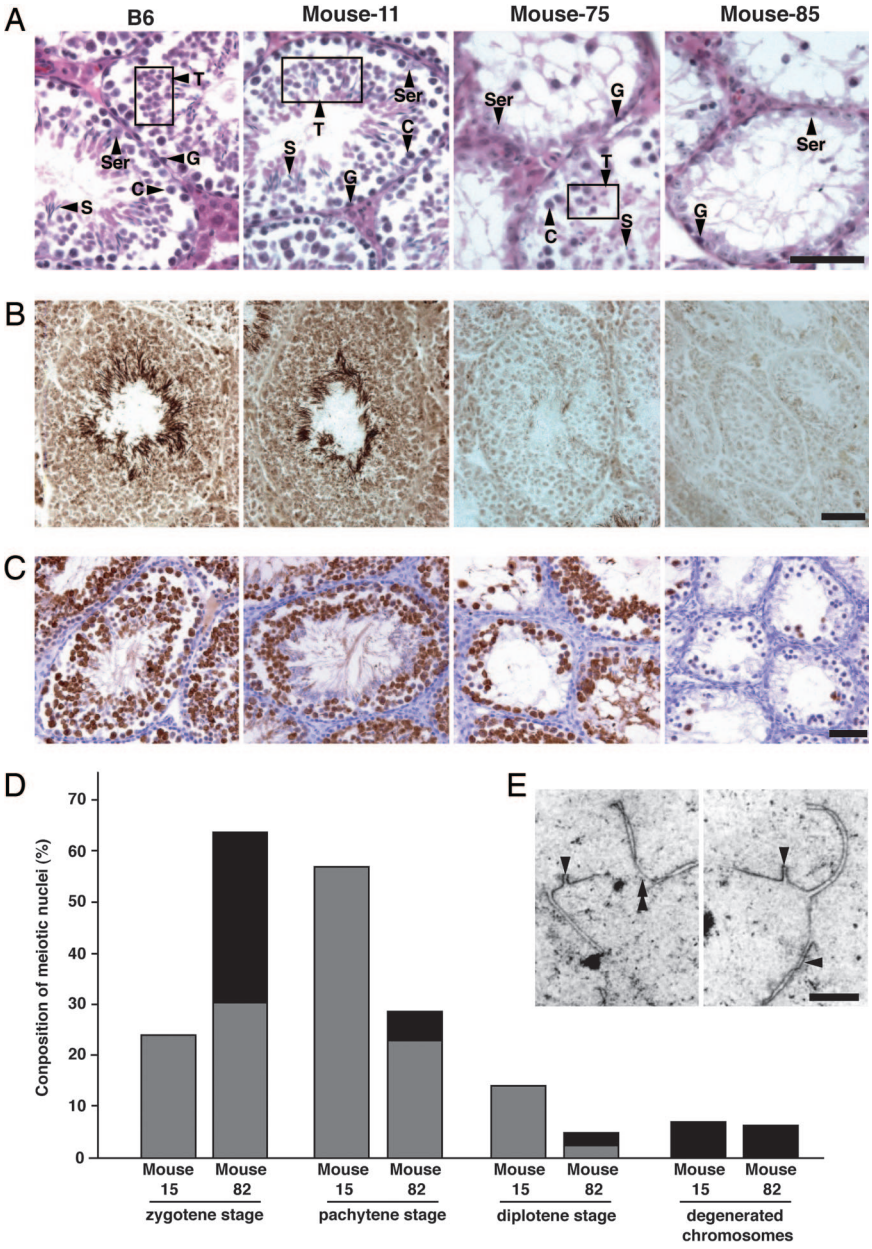

Fig. 3. Histopathological observations of testes from mito-mice. (*A*) Histological observations of testes. Testis sections from mouse-11 (group 1), -75 (group 2), -81 (group 3), and a B6 mouse were stained with H&E. G, spermatogonium; C, spermatocyte; T, spermatid; S, sperm; and Ser, Sertoli cell. The numbers of spermatocytes and spermatids were clearly decreased in mouse-75; in mouse-81 it is very difficult to identify any spermatocytes or spermatids. In mouse-75 and -85, spermatogonia were present but in slightly decreased numbers. (Scale bar: 50 μm.) (*B*) Mitochondrial respiratory function in testes. Cryosections from mouse-11 (group 1), -75 (group 2), -85 (group 3), and a B6 mouse were histochemically stained for COX activity, indicated by brown staining. In mouse-75 and -85, less COX staining was observed, indicating mitochondrial respiration dysfunction. (Scale bar: 50 μm.) (*C*) Distribution of MCA-positive cells in testes. Testis sections from mouse-11 (group 1), -75 (group 2), -85 (group 3), and a B6 mouse were stained with anti-MCA antiserum to visualize spermatocytes and spermatids. In mouse-75 and -85, the spermatocytes and spermatids were decreased in number, suggesting meiotic arrest. (Scale bar: 50 μm.) (*D*) Meiotic stages of nuclei in mito-mice. The meiotic nuclei from mouse-15 (group 1) and -82 (group 3) were categorized into the zygotene, pachytene, or diplotene stage by electron microscopy, and their frequencies are shown (gray bars). Because the nuclei with completely degenerated chromosomes could not be categorized into a stage, their frequencies are shown separately (black bars at the right). The frequencies of nuclei with partially fragmented and degenerated SCs are shown according to stage (black bars above gray bars). In mouse-82, the proportion of nuclei with partially fragmented and degenerated SCs was higher at the zygotene stage and low at pachytene stage, suggesting that spermatocytes with mitochondrial respiration defects caused by the accumulation of ΔmtDNA were arrested at the zygotene stage. (*E*) Homozygous chromosomes at the zygotene stage in mouse-82. Abnormal synapsis was seen in spermatocyte nuclei at the zygotene stage. Single and double arrowheads indicate the region with self-attachment and the degenerated SC, respectively. (Scale bar: 2 μm.)

meiotic chromosome analysis of spermatocytes isolated from mouse-15 (group 1) and -82 (group 3), and we observed the stage at which meiosis was arrested in mito-mice. In mouse-82, we observed a remarkable decrease in the spermatocyte population at the pachytene and diplotene stages compared with data from mouse-15, and most partially fragmented SCs were seen in spermatocyte nuclei at the zygotene stage (Fig. 3 *D* and *E*). Furthermore, abnormal and incomplete attachment was present in these spermatocyte nuclei (Fig. 3*E*). These results showed that in spermatocytes carrying high proportions of ΔmtDNA, meiosis was arrested at the zygotene stage because of abnormal synapsis, and it did not progress into the pachytene stage.

Because the increased number of spermatocytes with partially fragmented SCs suggested the possibility that spermatocytes underwent apoptosis, we examined whether apoptosis was enhanced in mito-mice groups 2 and 3. We observed more seminiferous tubules with terminal deoxynucleotidyltransferase-mediated dUTP nick end labeling (TUNEL)-positive cells in mito-mice groups 2 and 3 than in group 1 mito-mice or the B6 mice (Fig. 4*A*). In testes of mouse-74 (group 2) and -81 (group 3), TUNEL-positive spermatogenic cells increased in number in the region with the spermatocytes compared with results in mouse-9 (group 1) and B6 mouse testes (Fig. 4*B*). We also observed overexpression of caspase 3, one of the positive regulators in apoptosis pathway, in group 3 mito-mice compared with group 1 mito-mice (not shown). These results indicate that spermatogenic cells arrested at the zygotene stages were removed by apoptosis.

Discussion

Because mito-mice share the same nuclear–genomic background and genetically vary only in the proportions of pathogenic ΔmtDNA, they provide unambiguous evidence that the pathological phenotypes observed exclusively in the mito-mice carrying high accumulations of ΔmtDNA are caused by ΔmtDNA-induced respiration defects. Using these mito-mice, we succeeded in showing experimental evidence for mitochondria-related male infertility and in demonstrating that mitochondrial respiration activity is

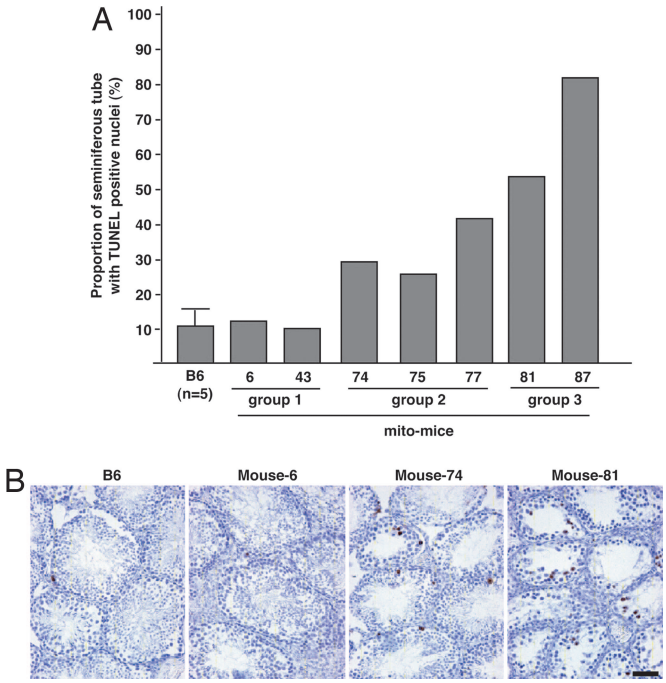

Fig. 4. Occurrence of apoptosis in testes of mito-mice. (*A*) Quantification of apoptosis by TUNEL staining in testis. In sections from mito-mice groups 1–3 (mouse-6, -43, -74, -75, -77, -81, and -87) and B6 mice ($n = 5$), frequencies of seminiferous tubules with TUNEL-positive cells are shown. Apoptosis was clearly more frequent in testes of mito-mice groups 2 and 3. (*B*) Distribution of TUNEL-positive cells in testes. Testis sections of mouse-6 (group 1), -74 (group 2), -81 (group 3), and a B6 mouse were stained with an apoptosis detection kit and counterstained with H&E. Brown and blue staining indicates TUNEL-positive and -negative nuclei, respectively. Small numbers of the TUNEL-positive cells were observed in mouse-6 and the B6 mouse. In mouse-74 and -81, the numbers of TUNEL-positive cells were clearly increased, and they tended to be distributed in the spermatocyte positions in the testis. (Scale bar: 50 μm.)

essential for mammalian spermatogenesis, especially for progression to the pachytene stages during meiosis and sperm formation. On the basis of these findings, we suggest that some cases of human male infertility with unknown etiology might result from mitochondrial respiratory dysfunction, although there are biological differences between human and mouse cases.

Possible pathophysiological mechanisms for mitochondria-related male infertility are as follows. When large amounts of pathogenic mutant mtDNA accumulate in testes, mitochondrial respiratory dysfunction is induced in spermatogenic cells. The reduction of energy production by the mitochondria induces meiotic arrest during spermatogenesis. In mito-mice carrying large amounts of ΔmtDNA, we observed a decrease in spermatocytes at the pachytene and diplotene stages and an increase in zygotene nuclei with partially fragmented and degenerated chromosomes (Fig. 3*D*). We also observed a higher frequency of cells undergoing apoptosis in the region of the testis with spermatocytes (Fig. 4*B*). Thus, respiration-deficient spermatocytes could not complete meiosis, and these cells were removed by apoptosis. Because the ΔmtDNA load differs in each cell (10, 12, 18), however, spermatocytes carrying a relatively lower proportion of ΔmtDNA can complete meiosis and transformation into haploid spermatids. These spermatids could differentiate into sperm, but most sperm showed intermediate COX activity (Fig. 2*A*) and abnormalities in middle piece and nucleus (Fig. 2*B*), suggesting abnormal sperm formation. Therefore, oligospermia and asthenozoospermia were induced by meiotic arrest and enhanced apoptosis during spermatogenesis and the generation of sperm with mitochondrial respiration deficiency and abnormal morphologies, respectively, resulting in male infertility. Because there is a possibility that sperm motility is sufficiently regulated by glycolysis (8), it was considered that asthenozoospermia in mito-mice was caused by morphological abnormalities rather than mitochondrial respiration deficiency in sperm. Although reactive oxygen species (ROS) are associated with asthenozoospermia and impaired fertility (for review, see ref. 20), the effect of ROS on sperm motility was not very great in mito-mice (unpublished data).

In addition, we found that the spermatogonia were present in testes of mito-mice groups 2 and 3 (Fig. 3 *A* and *C*), even when meiotic arrest had occurred, and spermatocytes, spermatids, and sperm were clearly reduced in number. The ΔmtDNA has a replication advantage because of its smaller size (9); therefore, the maintenance of mitotic spermatogonial division gives rise to additional accumulation of ΔmtDNA in spermatocytes, inducing further oligospermia and asthenozoospermia over time.

Considering that abnormal and incomplete attachment of homozygous chromosomes occurred only in mito-mice carrying large amounts of ΔmtDNA (Fig. 3*E*), the abnormalities of synapsis formation may be caused by energy deficiencies, resulting in meiotic arrest. It has been reported that synapsis of homozygous chromosomes in the mammalian spermatogenic meiotic process begins at the zygotene stage through chromosome movement and attachment (for reviews, see refs. 21 and 22) and that several factors for SCs, such as RAD51, DMC1, and cohesin, contain functional ATP-binding domains (23–25). In yeast, it has been demonstrated that mitochondrial respiratory function is essential for meiosis (13–15) and that mitochondrial dynamics determined by opposing mitochondrial fission and fusion events are important in the meiotic sporulation process (16). Our *in vivo* study using mito-mice, therefore, showed that it is possible that mitochondrial respiration defects induce abnormal attachment of homozygous chromosomes caused by dysfunction of indispensable factors for the SCs.

In our previous study, we obtained a normal number of progeny from female mito-mice carrying >70% ΔmtDNA, at least until they died at ≈6 months from mitochondrial diseases (9). Thus, in contrast to male mito-mice, females escape infertility, even when they carry large amounts of ΔmtDNA. This difference between sexes can be partly explained by the differences in meiotic cell division between oogenesis and spermatogenesis. In oogenesis, primary oocytes undergo meiosis synchronously at a late stage of embryogenesis, and all of the cells are suspended at the dictyotene stage before birth. During ovulation, a part of these primary oocytes resume meiosis and differentiate into mature oocytes. Therefore, we supposed that the synchronous onset of meiosis during embryogenesis forestalls the further accumulation of ΔmtDNA in primary oocytes, and consequently, oocytes carrying relatively lower amounts of ΔmtDNA are stably ovulated. Because mtDNA is inherited maternally (26), the mammalian female might have evolved the strategy of selecting only the healthy eggs, carrying relatively lower amounts of mutated mtDNA, by the synchronous onset of meiosis.

Our results implied several possible scientific and clinical applications. First, mito-mice are a very valuable model system for understanding the fundamental roles of mitochondrial respiratory function in the mammalian meiotic process because mito-mice are the only mammalian model with meiotic defects caused by mitochondrial respiratory dysfunction. Second, screening for sperm abnormalities would be effective for the early diagnosis of mitochondrial diseases. Unlike muscle biopsy for the diagnosis of mitochondrial diseases, this screening test would not be invasive, but it is suitable only for males. Finally, sperm samples from mito-mice could be used for screening drugs designed to restore mitochondrial respiratory dysfunction, based

on the recovery of decreased sperm motility. Compared with disease model mice generated by the manipulation of the nuclear genome, mito-mice are not always suitable for the drug screening because it is difficult to obtain a large population of mito-mice with the same ΔmtDNA load. However, the sperm samples from mito-mice could be used for large-scale drug screening. Moreover, drugs capable of improving mitochondrial respiratory dysfunction would be useful for treating not only mitochondrial diseases but also male infertility from mitochondrial causes.

Methods

Mice. Mice carrying ΔmtDNA, mito-mice, were generated by introducing ΔmtDNA from cultivated cells into zygotes of B6 strain mice (Crea Japan, Meguro, Tokyo, Japan) with cell-fusion techniques as described in ref. 9. Male mito-mice (4.5–6.5 months old) carrying various proportions of ΔmtDNA were used for the study. The proportion of ΔmtDNA in mito-mice was deduced from tail DNA samples because the proportions are very similar in all of the tissues of an individual mouse (9, 11, 17). Age-matched male B6 mice were also used as normal controls. Female B6 mice (2.0–4.0 months old) were used for the mating assay with the mito-mice and normal B6 mice.

Statistical Analysis. The data were analyzed with an unpaired Student's *t* test. All values are the means ± SD, and values with $P < 0.05$ were considered significant.

Mating Assay. Male mito-mice carrying various proportions of ΔmtDNA in their tails (7.0–86.6% ΔmtDNA) and age-matched male B6 mice were used in the assay. Groups 1 and 2 mito-mice were cohabitated with a female B6 mouse until a copulation plug was found in the female. Then the female with the plug was exchanged for a new female B6 mouse. The procedure was repeated at least three times. The number of progeny from each was counted. Even when group 3 mito-mice were cohabitated with female mice for >1 month, the copulation plugs were not found in the female.

Quantitative Estimation of ΔmtDNA. Proportions of wild-type and ΔmtDNA in tissues and sperm collected from mito-mice were determined by real-time detection PCR as described in ref. 17.

Assays for Sperm Number and Motility. Sperm samples collected from the cauda epididymidis of mito-mice and age-matched B6 mice were incubated in 500 μl of HTF medium, and the total sperm number was counted. These sperm samples were also used as samples for determining the ΔmtDNA content and for cytochemical staining for COX activity. Because the most sperm became active after 2 h of incubation and the activated sperm could swim up to the upper layer of the medium within the incubation time, the swim-up sperm were counted as the number of motile sperm after 2, 4, and 6 h of incubation.

***In Vitro* Fertilization Assay.** Mito-mice and B6 mice were induced to superovulate by consecutive injections of pregnant mare serum gonadotropin (Aska-Pharma, Minato, Tokyo, Japan) and human chorionic gonadotropin (hCG; Aska-Pharma) with an interval of 48 h between injections. Unfertilized oocytes were collected from the oviducts 15 h after the hCG injection. *In vitro* fertilization was carried out by using sperm collected from mito-mice and B6 mice in HTF medium in an incubator. After overnight incubation, the developmental frequency of two-cell-stage embryos was used as a measure of the rate of successful fertilization.

Histological Procedures. Testes from mito-mice and B6 mice were fixed in 10% formaldehyde solution. Paraffin sections (6 μm thick) of the testes were stained with hematoxylin/eosin (H&E). Sections were also stained by indirect immunostaining with an anti-MCA antiserum (18) followed by a secondary antibody, rhodamine-conjugated goat anti-IgGs (H+L) (Jackson ImmunoResearch Laboratories, West Grove, PA). The sections stained with anti-MCA antiserum were counterstained with H&E to visualize all nuclei. A TUNEL staining assay was performed with an *in situ* apoptosis detection kit (TaKaRa Bio, Otsu, Shiga, Japan) according to the manufacturer's instructions. The stained sections were counterstained with H&E to visualize all nuclei. Histochemical and cytochemical analyses for COX activity were carried out as described in refs. 9 and 11. Frozen sections (10 μm thick) of testes and sperm mounted on glass slides were used as samples for the analyses.

Meiotic Chromosome Analysis. The meiotic chromosome analysis was performed with a method described in ref. 27. Briefly, the spermatogenic cells prepared from testes of mito-mice were dispersed, the nuclei were stained with 50% silver nitrate, and the samples were analyzed under an electron microscope. On the basis of differences in chromosomal synapsis formation, spermatocyte nuclei were classified as being at the zygotene, pachytene, or diplotene stage or as degenerated cells, and the percentage frequencies of each stage and of degenerated cells were calculated.

We thank Drs. K. Yamagata and K. Miyado for technical advice and critical discussions. This work was supported by Grant-in-Aid for Young Scientists 17689023 from the Japan Society for Promotion of Science (to K.N.); by Research Grant 17A-10 for Nervous and Mental Disorders from the Ministry of Health, Labor, and Welfare (to K.N.); and by Grant-in-Aid 14GS0305 for Creative Scientific Research from the Ministry of Education, Culture, Sports, Science, and Technology of Japan (to J.-I.H.).

1. Wallace DC (1999) *Science* 283:1482–1488.
2. Folgero T, Bertheussen K, Lindal S, Torbergsen T, Oian P (1993) *Hum Reprod* 8:1863–1868.
3. Spiropoulos J, Turnbull DM, Chinnery PF (2002) *Mol Hum Reprod* 8:719–721.
4. Kao S-H, Chao H-T, Wei Y-H (1995) *Biol Reprod* 52:729–736.
5. Lestienne P, Reynier P, Chretien MF, Penisson-Besnier I, Malthiery Y, Rohmer V (1997) *Mol Hum Reprod* 3:811–814.
6. Carra E, Sangiorgi D, Gattuccio F, Rinaldi AM (2004) *Biochem Biophys Res Commun* 322:333–339.
7. Ruiz-Pesini E, Diez C, Lapena AC, Perez-Martos A, Montoya J, Alvarez E, Arenas J, Lopez-Perez MJ (1998) *Clin Chem* 44:1616–1620.
8. Miki K, Qu W, Goulding EH, Willis WD, Bunch DO, Strader LF, Perreault SD, Eddy EM, O'Brien DA (2004) *Proc Natl Acad Sci USA* 101:16501–16506.
9. Inoue K, Nakada K, Ogura A, Isobe K, Goto Y-i, Nonaka I, Hayashi J-I (2000) *Nat Genet* 26:176–181.
10. Holt IJ, Harding A, Morgan-Hughes JA (1988) *Nature* 331:717–719.
11. Nakada K, Inoue K, Ono T, Isobe K, Ogura A, Goto Y-i, Nonaka I, Hayashi J-I (2001) *Nat Med* 7:934–940.
12. Nakada K, Sato A, Sone H, Kasahara A, Ikeda K, Kagawa Y, Yonekawa H, Hayashi J-I (2004) *Biochem Biophys Res Commun* 323:175–184.
13. Kuenzi MT, Tingle MA, Halvorson HO (1974) *J Bacteriol* 117:80–88.
14. Marmiroli N, Ferri M, Puglisi PP (1983) *J Bacteriol* 154:118–129.
15. Treinin M, Simchen G (1993) *Curr Genet* 23:223–227.
16. Gorsich SW, Shaw JM (2004) *Mol Biol Cell* 15:4369–4381.
17. Sato A, Kono T, Nakada K, Ishikawa K, Inoue S-I, Yonekawa H, Hayashi J-I (2005) *Proc Natl Acad Sci USA* 102:16765–16770.
18. Tsuchida J, Nishina Y, Wakabayashi N, Nozaki M, Sakai Y, Nishimune Y (1998) *Dev Biol* 197:67–76.
19. Page SL, Hawley RS (2004) *Annu Rev Cell Dev Biol* 20:525–558.
20. Ford WCL (2001) *Lancet* 357:1223–1224.
21. Barton NR, Goldstein LSB (1996) *Proc Natl Acad Sci USA* 93:1735–1742.
22. Cobb J, Handel MA (1998) *Semin Cell Dev Biol* 9:445–450.
23. Morita T, Yoshimura Y, Yamamoto A, Murata K, Mori M, Yamamoto H, Matsushiro A (1993) *Proc Natl Acad Sci USA* 90:6577–6580.
24. Habu T, Taki T, West A, Nishimune Y, Morita T (1996) *Nucleic Acids Res* 24:470–477.
25. Anderson DE, Losada A, Erickson HP, Hirano T (2002) *J Cell Sci* 156:419–424.
26. Kaneda H, Hayashi J-I, Takahama S, Taya C, Fischer Lindahl K, Yonekawa H (1995) *Proc Natl Acad Sci USA* 92:4542–4546.
27. Yoshida K, Kondoh G, Matsuda Y, Habu T, Nishimune Y, Morita T (1998) *Mol Cell* 1:707–718.